

# Indirect exchange interaction between two quantum dots in an Aharonov-Bohm ring

Yasuhiro Utsumi,<sup>1</sup> Jan Martinek,<sup>2,3,4</sup> Patrick Bruno,<sup>1</sup> and Hiroshi Imamura<sup>5</sup>

<sup>1</sup>Max-Planck-Institut für Mikrostrukturphysik, Weinberg 2, D-06120 Halle (Saale), Germany

<sup>2</sup>Institut für Theoretische Festkörperphysik, Universität Karlsruhe, 76128 Karlsruhe, Germany

<sup>3</sup>Institute for Materials Research, Tohoku University, Sendai 980-8577, Japan

<sup>4</sup>Institute of Molecular Physics, Polish Academy of Sciences, 60-179 Poznań, Poland

<sup>5</sup>Graduate School of Information Sciences, Tohoku University, Sendai 980-8579, Japan

(Received 19 July 2003; revised manuscript received 3 December 2003; published 22 April 2004)

We investigate the Ruderman-Kittel-Kasuya-Yosida (RKKY) interaction between two spins located at two quantum dots embedded in an Aharonov-Bohm (AB) ring. In such a system the RKKY interaction, which oscillates as a function of the distance between two local spins, is affected by the flux. For the case of the ferromagnetic RKKY interaction, we find that the amplitude of AB oscillations is enhanced by the Kondo correlations and an additional maximum appears at half flux, where the interaction is switched off. For the case of the antiferromagnetic RKKY interaction, we find that the phase of AB oscillations is shifted by  $\pi$ , which is attributed to the formation of a singlet state between two spins for the flux value close to integer value of flux.

DOI: 10.1103/PhysRevB.69.155320

PACS number(s): 73.23.Hk, 75.20.Hr

## I. INTRODUCTION

When two magnetic moments are embedded in a metal, they induce spin polarization in a conduction electron sea and couple each other even if they are spatially separated. Such indirect exchange interaction, the Ruderman-Kittel-Kasuya-Yosida (RKKY) interaction, has been known from the 1950s.<sup>1</sup> The indirect exchange interaction in magnetic nanostructures is one of basic mechanisms for spintronics<sup>2</sup> and it is well understood for ferromagnet and nonmagnetic metal multilayer structures.<sup>3</sup> However for semiconductor nanostructures, the indirect exchange interaction between local spins formed in two quantum dots has not yet been observed, in spite of the importance as a basic physics and the potential application for semiconductor nanospintronics.

Recent improvement of the fabrication technique for semiconductor nanostructures enables one to make rather complicated structures with the possibility of the precise controlling of their parameters. For example, a double quantum dot (QD) system<sup>4</sup> and the composite system of QD and an Aharonov-Bohm (AB) ring have been made.<sup>5,6</sup> The double-dot system was proposed for a candidate of “qubits,” because in the Coulomb blockade (CB) regime a dot with odd numbers of electrons, behaves as a local spin and two dot spins can be entangled by introducing the exchange interaction between them.<sup>7</sup> Such exchange interaction has been also discussed from the point of view of the competition between the Kondo effect and the antiferromagnetic (AF) interaction.<sup>8</sup> However the direct exchange interaction was considered rather than the RKKY interaction. Investigations on the AB ring embedded with QD are aimed at understanding the coherent transport through QD (Refs. 5,9 and 10) and the indirect exchange interaction between two local spins has not been addressed.

So it is intriguing to investigate the RKKY interaction between two QD's in CB regime embedded in AB ring. We will show that the RKKY interaction, the sign of which oscillates as a function of the distance (RKKY oscillations), is affected by the flux and it dominates the transport properties.

For ferromagnetic (F) coupling between dot spins, the amplitude of AB oscillations is enhanced by Kondo correlations and an additional maximum appears at half flux. For AF coupling case, the phase of AB oscillations is shifted by  $\pi$ .

## II. MODEL AND CALCULATIONS

### A. Model Hamiltonian

Figure 1(a) shows the schematic picture of an AB ring embedded with one QD in each arm. They are formed in a two-dimensional electron gas (2DEG) by means of gate voltages. QD's denoted by 1 and 2 weakly couple to left and right leads, which are connected strongly to reservoirs. In order to discuss RKKY interaction, we need to consider the situation when each quantum dot is occupied by odd number of electrons, so both of them are in the local moment regime. The leads can include several channels depending on their width. In the following for simplicity, we will assume the

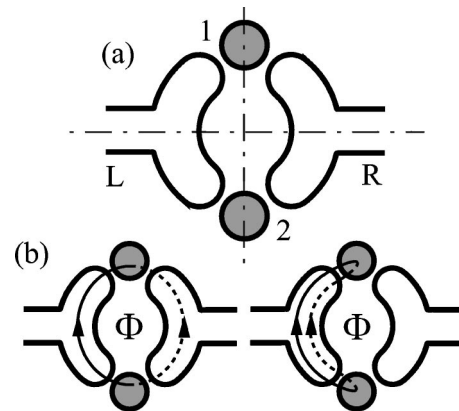


FIG. 1. (a) Aharonov-Bohm ring embedded with one QD in each arm. The system has the parity symmetry along the horizontal and vertical axes (dot-dashed lines). (b) The flux dependent (left panel) and independent (right panel) particle-hole excitation.  $\Phi$  is the flux penetrating the ring. The directed solid and dashed lines are the particle and hole propagators, respectively.

single-channel case. The effective Hamiltonian of such system may be written with two one-dimensional (1D) leads Hamiltonian  $H_0$  and the tunneling Hamiltonian  $H_T$  as  $H = H_0 + H_T$ . The lead Hamiltonian is given by  $H_0 = \sum_{k,r=L,R} \sigma \varepsilon_k a_{kr\sigma}^\dagger a_{kr\sigma}$ , where  $a_{kL(R)\sigma}$  is an annihilation operator of an electron with quantum number  $k$  and spin  $\sigma$  in the left (right) lead. For simplicity, we adopt the so-called Coqblin-Schrieffer model,

$$H_T = \sum_{\substack{r,r'=L,R \\ n=1,2}} \sum_{\sigma,\sigma'=\uparrow,\downarrow} \frac{J}{2} a_{rn\sigma}^\dagger X_{\sigma'}^n a_{r'n\sigma'}, \quad (1)$$

for the tunneling Hamiltonian through QD's with odd numbers of electrons in CB regime. The Hubbard operator  $X_{\sigma'}^n \equiv |n, \sigma'\rangle \langle n, \sigma|$  describes the spin state of the  $n$ -th QD and  $J > 0$  is a coupling constant. The annihilation operator  $a_{rn\sigma}$  is written using the projection  $\langle n|kr\rangle$  of wave function of an electron in the lead  $r$  with quantum number  $k$  at the boundary of the  $n$ th QD, as  $a_{rn\sigma} \equiv \sum_k \langle n|kr\rangle a_{kr\sigma}$ .<sup>11</sup>

Here we encounter a problem: One needs to know the proper wave function including the information on the coherent propagation of an electron through the arms. Though the scattering theory<sup>12</sup> is suitable for treating the electron coherence, it is complicated to combine it with a theory based on the Hamiltonian in the second-quantization representation, i.e., the tunnel Hamiltonian approach.<sup>13</sup> In this paper we circumvent this problem. Rather, we utilize an assumption of parity (mirror) symmetry along the horizontal and the vertical axes [dot-dashed lines in Fig. 1(a)]; namely, the total Hamiltonian is invariant under the interchange of indices  $L \leftrightarrow R$  or  $1 \leftrightarrow 2$ . Such an approximation will make calculations simple and will contain all important physics. Any deviations from such a symmetry will change the result only quantitatively.

For practical calculations, it is convenient to introduce an annihilation operator of even/odd parity states<sup>14</sup>  $a_{r\pm\sigma} = (a_{r1\sigma} \pm a_{r2\sigma})/\sqrt{2}$  [ $a_{r\pm\sigma} = \sum_k \langle \pm|k\rangle a_{kr\sigma}$ , where  $|\pm\rangle = (|1\rangle \pm |2\rangle)/\sqrt{2}$ ; we dropped the index  $r$  from  $|kr\rangle$  because of the parity symmetry along the vertical axis]. Annihilation operators for even and odd parity states are orthogonal,

$$\{a_{rp\sigma}, a_{r'p'\sigma'}\} = \delta_{rr'} \delta_{\sigma\sigma'} \delta_{pp'}, \quad (2)$$

because of the parity symmetry along the horizontal axis.

When magnetic field is applied, an AB phase factor  $e^{i\phi/2}$  ( $e^{-i\phi/2}$ ) must be counted in Eq. (1), when electron tunnels through a QD in the clockwise (anticlockwise) direction.<sup>15</sup>

The AB phase is written with vector potential  $\vec{A}$  as,

$$\phi = 2\pi \frac{\Phi}{\Phi_0}, \quad \Phi = \oint \vec{A} \cdot d\vec{l}, \quad (3)$$

where  $\Phi_0 = hc/e$  is the flux quantum and the line integral is performed along the ring in the clockwise direction. An AB flux breaks the time-reversal symmetry and it generates the main difference between features of the orthodox two-impurity Kondo model<sup>14,16-19</sup> and the AB ring embedded with one QD in each arm. Here, we note that the magnetic field in leads and QD's is not zero for an experiment and it

causes Zeeman splitting of electron spins. In the following discussions, we consider an ideal situation where the Zeeman splitting is negligible. As we comment in Sec. IV B, such a situation will be typical for materials with a small Landé  $g$  factor.

## B. Flux dependent RKKY interaction

The Hamiltonian for the RKKY interaction can be obtained by the second order perturbation theory in terms of  $J/\varepsilon_F$ , where  $\varepsilon_F$  is the Fermi energy.<sup>1,20</sup>

$$H_{\text{RKKY}} = \frac{J_{\text{RKKY}}(\phi)}{2} \sum_{\sigma\sigma'} X_{\sigma\sigma'}^1 X_{\sigma'\sigma}^2. \quad (4)$$

The coupling constant  $J_{\text{RKKY}}(\phi)$  can be written as

$$J_{\text{RKKY}}(\phi) = \frac{J^2}{2} \chi(2 + 2 \cos \phi), \quad (5)$$

where a susceptibility function  $\chi$  can be found by the perturbation theory based on the Keldysh Green function technique.<sup>20</sup> In the equilibrium, it can be written as

$$J^2 \chi = \sum_p \frac{1}{4} \text{Re} \int d\varepsilon d\varepsilon' \frac{\gamma_p(\varepsilon) \gamma_p(\varepsilon') - \gamma_p(\varepsilon) \gamma_{\bar{p}}(\varepsilon')}{\varepsilon + i\eta - \varepsilon'} \times \{f^+(\varepsilon) - f^+(\varepsilon')\}, \quad (6)$$

where  $\eta$  is a positive infinitesimal number and  $\gamma_p(\varepsilon) = J \sum_k \langle p|k\rangle \langle k|p\rangle \delta(\varepsilon - \varepsilon_k)$  is a spectral function of parity  $p$  "electron propagator." The subscript  $\bar{p}$  represents the opposite parity of  $p$ , i.e.,  $\bar{p} = \pm$  for  $p = \mp$ . Here,  $f^\pm(\varepsilon) = 1/(1 + e^{\pm\beta\varepsilon})$  is the electron (hole) distribution function, and  $\beta \equiv T^{-1}$ , (We use the unit  $k_B \equiv 1$ .) In Eq. (5), a phase dependent factor  $(2 + 2 \cos \phi)$  appears, which is related to the four configurations of particle-hole excitations—two of which enclose the flux [left panel of Fig. 1(b)] and pick up a phase factor  $e^{i\phi}$  or  $e^{-i\phi}$  and give term  $2 \cos \phi$ , and the others (right panel) are independent of the flux and give term 2. Equation (5) is one of the main results of this paper. It shows that by means of external flux  $\phi$  one can control the amplitude of the RKKY interaction but it is impossible to change its sign since  $(2 + 2 \cos \phi) \geq 0$ .

Since we consider 1D leads, we approximate  $\gamma_p(\varepsilon)$  as for the 1D free-electron gas with the linearized dispersion relation:<sup>14</sup>

$$\gamma_\pm(\varepsilon) \approx \bar{J} \left[ 1 \pm \cos \left\{ k_F l \left( 1 + \frac{\varepsilon}{D} \right) \right\} \right], \quad (7)$$

where  $k_F$  is the Fermi wave number and  $l$  is the length of an electron path between two QD's. The argument of cosine function is the energy dependent "orbital phase,"<sup>21</sup> i.e., the accumulated phase during electron propagation between two QD's. We introduced the cutoff energy  $D = \hbar v_F k_F$ , where  $v_F$  is the Fermi velocity. Here,  $\bar{J}$  is written with the density of states  $\rho$  as  $\bar{J} \equiv J\rho$ .

Substituting Eq. (7) into Eqs. (5) and (6), we obtain for short distance between two QD's ( $k_F l \ll 2\pi$ ) the ferromag-

netic coupling as  $J_{\text{RKKY}}(\phi) \approx -2 \ln 2 \bar{J} D (2 + 2 \cos \phi)$  and, more relevant, the RKKY oscillations of 1D free-electron gas<sup>1,22</sup> as a function of  $l$  for long distance between dots ( $k_{\text{F}} l \gg 2\pi$ ),

$$J_{\text{RKKY}}(\phi) \approx -\frac{\pi \bar{J}^2 D \cos(2k_{\text{F}} l)}{4 k_{\text{F}} l} (2 + 2 \cos \phi). \quad (8)$$

Above expressions are obtained by replacing the Fermi functions in Eq. (6) with those at  $T=0$ , which is valid below the characteristic temperature  $T^*$  defined by

$$T^* \equiv \frac{\hbar}{\tau}, \quad \tau \equiv \frac{\hbar k_{\text{F}} l}{D} = \frac{l}{v_{\text{F}}}. \quad (9)$$

Here,  $\tau$  is the characteristic time scale for an electron traveling between two QD's. It can be understood from the following argument: Electrons deep inside the Fermi sea are responsible for the RKKY oscillations. On the other hand, electrons with energy  $\varepsilon$  ( $|\varepsilon| \ll T^*$ ), i.e., electrons around the Fermi level, are unimportant, because such electrons contribute only oscillations whose characteristic wave length  $\hbar v_{\text{F}}/T^*$  is much longer than  $l$ . Thus the RKKY oscillations are insensitive to the temperature in the regime  $T \ll T^*$ . However, when the temperature reaches  $T^*$ , the RKKY oscillations are affected by the thermal excitations of lead electrons and will be smeared out.

Due to the RKKY interaction, depending on the sign of the coupling  $J_{\text{RKKY}}(\phi)$  [Eq. (8)], the two dot spins are entangled and form a singlet state  $|0,0\rangle$  for AF coupling [ $J_{\text{RKKY}}(\phi) > 0$ ] or a triplet state  $|1,m\rangle$  ( $m=0, \pm 1$ ) for F coupling [ $J_{\text{RKKY}}(\phi) < 0$ ].

We should note the limitation of the above approximation. Equation (7) may not count the influence of the potential barrier at the boundary of QD's and the shape of junctions between leads and reservoirs on an electron wave function. Thus, in reality, the RKKY oscillations would be modified, however our main result, the flux dependent RKKY interaction, Eq. (5), will not be much affected by such an approximation.

### C. Conductance

In the following, we will discuss how the flux dependent RKKY interaction affects the conductance. The effect of the RKKY interaction would be pronounced below the temperature  $T \approx |J_{\text{RKKY}}(0)|$ . In this regime, it might be unrealistic to ignore Kondo correlations, which grow already much above the Kondo temperature  $T_{\text{K}} \approx D \exp\{-1/(2\bar{J})\}$  and cause the logarithmic variation of transport properties with temperature already above  $T_{\text{K}}$ .<sup>23</sup> In the following, we will calculate the conductance for  $|J_{\text{RKKY}}(0)| \gg T_{\text{K}}$  and will take into account Kondo correlations within the third-order perturbation theory in terms of  $\bar{J}$ .

First we rewrite the tunnel Hamiltonian, Eq. (1), using the vector operator of the  $n$ th local spin  $\vec{S}^n$ , whose components are defined as  $S_{+/-}^n = X_{\uparrow/\downarrow}^n$  and  $S_z^n = (X_{\uparrow}^n - X_{\downarrow}^n)/2$ . Further we introduce operators  $\vec{S}^{\pm} = \vec{S}^1 \pm \vec{S}^2$ , which satisfy the following commutation relations:

$$[S_i^p, S_j^p] = i \epsilon_{ijk} S_k^+, \quad [S_i^p, S_j^{\bar{p}}] = i \epsilon_{ijk} S_k^-, \quad (10)$$

where  $\epsilon_{ijk}$  is the Levi-Chivita antisymmetric tensor. The operator  $\vec{S}^+$  does not change the total spin-quantum number, while  $\vec{S}^-$  is the operator of the singlet-triplet transition. By using above operators, we obtain the symmetrized form of  $H_{\text{T}}$ <sup>16,24,14</sup> taking into account the AB phase as

$$H_{\text{T}} = \frac{J}{4} \sum_{\substack{p=\pm \\ \sigma, \sigma'=\uparrow, \downarrow}} \left\{ \sum_r (\vec{\sigma}_{rr}^p \cdot \vec{S}^p + v a_{rp\sigma}^\dagger \delta_{\sigma' \sigma} a_{rp\sigma}) \right. \\ + \cos \frac{\phi}{2} (\vec{\sigma}_{RL}^p \cdot \vec{S}^p + v a_{Rp\sigma}^\dagger \delta_{\sigma' \sigma} a_{Lp\sigma}) + \text{H.c.} \\ \left. + i \sin \frac{\phi}{2} (\vec{\sigma}_{RL}^{\bar{p}} \cdot \vec{S}^p + v a_{R\bar{p}\sigma}^\dagger \delta_{\sigma' \sigma} a_{Lp\sigma}) + \text{H.c.} \right\}. \quad (11)$$

Here,  $\vec{\sigma}_{r'r}^{+(-)} = \sum_{\sigma\sigma'p} a_{r'p\sigma}^\dagger \vec{\sigma}_{\sigma'\sigma} a_{rp(\bar{p})\sigma}$  denotes effective conducting electron spin and is defined with the vector Pauli matrix  $\vec{\sigma}$ . Terms proportional to  $v$  represent potential scattering process and for our case,  $v=1$ . The first line represents the reflection process and shows that the change of parity and the singlet-triplet transition occur simultaneously. The second and the third lines describe transmission processes. The third line describes the singlet-triplet transition without changing the parity, which is not invariant under the interchange of indices,  $L \leftrightarrow R$ , or  $1 \leftrightarrow 2$ , (i.e., the replacement of  $a_{r\pm\sigma}$  with  $\pm a_{r\pm\sigma}$ ). Here it does not mean that the parity symmetry is broken by the flux: the space inversion transformation changes  $\phi \rightarrow -\phi$ , because it also reverses the direction of the line integral in Eq. (3).

In order to calculate the linear conductance, we adopt the diagrammatic technique for the density matrix in the real-time domain.<sup>25,26</sup> With the help of the commutation relations, Eq. (10), the perturbative calculation is performed rather systematically (see the Appendix). The ‘‘partial self-energy’’ which represents the transition rate for an electron from the left lead to the right lead accompanied by the triplet-triplet transition  $\Sigma_{11}^{LR}$  preserving a singlet state  $\Sigma_{00}^{LR}$  or accompanied by the singlet-triplet transition  $\Sigma_{j\bar{j}}^{LR}$  ( $j=0,1$ ) is obtained as follows:

$$\Sigma_{11}^{LR} \approx \frac{3\pi i}{2} \int d\varepsilon \sum_{p=\pm} \left[ \gamma_{pL}^+(\varepsilon) \gamma_{pR}^-(\varepsilon) \text{Re} \left\{ 1 + \frac{v^2}{2} + \sigma_{1p}(\varepsilon) \right. \right. \\ \left. \left. + \sum_{j=0,1} \frac{\sigma_{1\bar{j}}(\varepsilon - \Delta_{j\bar{j}})}{2} \right\} \cos^2 \frac{\phi}{2} + \gamma_{pL}^+(\varepsilon) \gamma_{\bar{p}R}^-(\varepsilon) \right. \\ \left. \times \text{Re} \left\{ 1 + \frac{v^2}{2} + \sigma_{0p}(\varepsilon) + \sum_{j=0,1} \frac{\sigma_{0\bar{j}}(\varepsilon - \Delta_{j\bar{j}})}{2} \right\} \sin^2 \frac{\phi}{2} \right], \quad (12)$$

$$\Sigma_{00}^{LR} \approx \frac{\pi i}{4} \int d\varepsilon \sum_{p=\pm} v^2 \left\{ \gamma_{pL}^+(\varepsilon) \gamma_{pR}^-(\varepsilon) \cos^2 \frac{\phi}{2} + \gamma_{pL}^+(\varepsilon) \gamma_{pR}^-(\varepsilon) \sin^2 \frac{\phi}{2} \right\}, \quad (13)$$

$$\Sigma_{jj}^{LR} \approx \frac{3\pi i}{4} \int d\varepsilon \sum_{p=\pm} \left[ \gamma_{pL}^+(\varepsilon) \gamma_{pR}^-(\varepsilon - \Delta_{\bar{j}j}) \operatorname{Re}\{1 + \sigma_{1p}(\varepsilon) + \sigma_{1\bar{p}}(\varepsilon - \Delta_{\bar{j}j})\} \cos^2 \frac{\phi}{2} + \gamma_{pL}^+(\varepsilon) \gamma_{pR}^-(\varepsilon - \Delta_{\bar{j}j}) \times \operatorname{Re}\{1 + \sigma_{0p}(\varepsilon) + \sigma_{0\bar{p}}(\varepsilon - \Delta_{\bar{j}j})\} \sin^2 \frac{\phi}{2} \right], \quad (14)$$

where we neglected the integral  $\operatorname{Re} \int d\varepsilon' \gamma_p(\varepsilon') / (\varepsilon + i\eta - \varepsilon')$ . The subscript  $j=1(0)$  denotes the total-spin quantum number and  $\bar{j}=0(1)$ . Here  $\Delta_{10} = -\Delta_{01} = J_{\text{RKKY}}(\phi)$  and  $\gamma_{pr}^{\pm}(\varepsilon) = \gamma_p(\varepsilon) f^{\pm}(\varepsilon - \mu_r)$  denotes the ‘‘lesser’’ or ‘‘greater’’ Green function where  $\mu_L = -\mu_R = eV/2$ . The function  $\sigma_{0(1)p}$  defined by

$$\sigma_{0(1)p}(\varepsilon) = \int d\varepsilon' \frac{\gamma_p^+(\varepsilon') + \gamma_{p(p)R}^+(\varepsilon')}{\varepsilon + i\eta - \varepsilon'} \quad (15)$$

gives the logarithmic divergence related with Kondo correlations. By substituting Eq. (7) into Eq. (15), we obtain

$$\sigma_{0\pm}(\varepsilon) \approx 2\bar{J} \ln \frac{2e\gamma D}{\pi T},$$

$$\sigma_{1\pm}(\varepsilon) \approx \sigma_{0\pm}(\varepsilon) \pm 2\bar{J} \operatorname{Re} \left[ e^{ik_{\text{F}}l} \left\{ \ln \frac{2T^*}{\pi T} + \operatorname{Ei}(-ik_{\text{F}}l) \right\} \right],$$

for  $V=0$  and  $\varepsilon \ll T, T^*$ . Here  $\operatorname{Ei}(x)$  denotes the exponential integral function and  $\gamma \approx 0.577$  is the Euler constant. Equation (5) supplemented with Eq. (6) and Eqs. (12)–(14) are main results of this paper.

Using the partial self-energy, Eqs. (12)–(14), the current can be expressed as

$$I = -\frac{ie}{\hbar} \sum_{j,j'=0,1} P_j \{ \Sigma_{jj'}^{LR} - (L \leftrightarrow R) \}, \quad (16)$$

where probabilities  $P_0$  for a singlet state and  $P_1$  for each of particular triplet states (we consider no Zeeman splitting) can be obtained for the linear response from the Boltzmann distribution as

$$P_0 = \frac{1}{1 + 3 \exp[-\beta J_{\text{RKKY}}(\phi)]}, \quad P_1 = \frac{1 - P_0}{3}. \quad (17)$$

The linear conductance is defined as  $G = \lim_{V \rightarrow 0} \partial I / \partial V$ .

### III. RESULTS

For the AB ring geometry without quantum dots in arm, the conductance oscillates as a function of the flux  $\phi$ .<sup>12</sup> Furthermore, because of the orbital phase, the conductance also oscillates as a function of the length of the arm  $l$  for enough

low temperatures: As the thermal excitation of lead electrons scrambles various orbital phases, the oscillatory component would be reduced for temperatures above the characteristic temperature  $T^*$ , where characteristic length  $\hbar v_{\text{F}}/T$  reaches  $l$ . When one local spin, i.e., QD, is embedded in each arm of the AB ring, in addition to the oscillatory component, the nonoscillatory background of oscillations related to spin-flip processes will appear: Spin-flip processes do not contribute to the interference effect<sup>27</sup> because if a local spin is flipped, we can determine the path which an electron propagated. Such nonoscillatory background reduces the portion of oscillatory component. However, if we take account of the RKKY interaction, the oscillatory component can be enhanced from the following mechanism: First, according to Eq. (17), the probabilities for singlet  $P_0$  and triplet  $P_1$  states will be affected by the RKKY coupling constant  $J_{\text{RKKY}}(\phi)$ , which is an oscillatory function in terms of  $\phi$  and  $l$ . Second, as the conductance would be sensitive to a state of local spins, it would show also the oscillatory behavior related to the oscillations of  $J_{\text{RKKY}}(\phi)$ . Such RKKY dominant oscillations one could expect for the enough low temperature  $T \ll |J_{\text{RKKY}}(0)| \ll T^*$ .

In the following, we will discuss the properties of our system for temperatures where the thermal scrambling of orbital phases is unimportant  $T \ll T^*$  and above the Kondo temperature  $T > T_{\text{K}}$ . We note that as  $|J_{\text{RKKY}}(\phi)| \ll T^*$ , the modification of orbital phases by inelastic spin-flip scattering events is also unimportant.

#### A. $l$ dependence

First we will discuss the RKKY oscillations without magnetic flux  $\phi=0$  as a function of the distance  $l$  between two QD's. Figure 2(a) shows the RKKY oscillations of the coupling constant  $J_{\text{RKKY}}(0)$  as a function of the length of an electron path  $l$  obtained using Eq. (8). It oscillates with the period of  $k_{\text{F}}l/\pi = 1$ , and shows local minima at integer values of  $k_{\text{F}}l/\pi$  corresponding to F coupling and local maxima at half-integer values of  $k_{\text{F}}l/\pi$  corresponding to the AF coupling between the spins. The amplitude of the oscillations decays with  $1/k_{\text{F}}l$  as predicted for RKKY interaction in quasi-1D geometry.<sup>22</sup> In Fig. 2(b), there is a plot of the probability  $P_0$  of the singlet state obtained from Eq. (17). At low temperature  $T \lesssim |J_{\text{RKKY}}(0)|$  (the solid line), a singlet state (triplet state) is formed when value of  $k_{\text{F}}l/\pi$  is close to half integer (integer). As the temperature increases [the dashed line for  $T \sim |J_{\text{RKKY}}(0)|$  and the dotted line for  $T \gg |J_{\text{RKKY}}(0)|$ ] the amplitude of oscillations is suppressed and system approaches uniform distribution between the singlet and triplet states— $P_0 = P_1 = 1/4$ . There are also the oscillations of the conductance [Fig. 2(c)] with the period of  $k_{\text{F}}l/\pi = 1$ . In the same way as in Fig. 2(b), the amplitude of oscillations is suppressed for  $T \gg |J_{\text{RKKY}}(0)|$ , which indicates that in the regime  $T < |J_{\text{RKKY}}(0)|$  the conductance oscillations are mainly determined by the RKKY interaction. Experimentally, it can be difficult to control the length of arms keeping other parameters fixed. However, the conductance oscillations would be possible to observe by changing

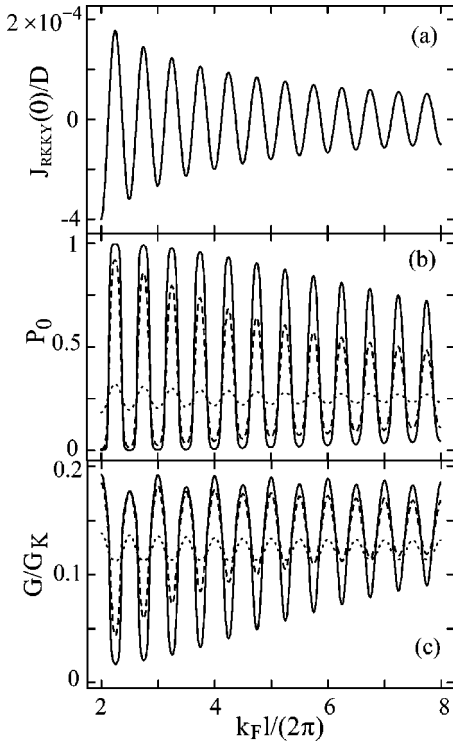


FIG. 2. Length dependent (a) RKKY coupling constant, (b) probability for singlet state, and (c) conductance for  $T/D=5 \times 10^{-5}$  (solid line),  $10^{-4}$  (dashed line), and  $10^{-3}$  (dotted line). Parameters are taken as  $\phi=0$  and  $\bar{J}=0.04$ .

the Fermi wave number  $k_F$ , by controlling the carrier density of 2D electron gas with an additional gate.

### B. $\phi$ dependence, analytical results

Though above discussions suggest that the RKKY interaction dominates the length dependent conductance, it would be more convenient experimentally to measure the flux dependence. In the following we will discuss the modification of AB conductance oscillations by the presence of RKKY interaction.

As we mentioned before by means of external flux  $\phi$  one can change the amplitude of the RKKY interaction but not its sign since  $(2+2\cos\phi) \geq 0$ . In the particular experimental situation depending on the length  $l$  of the arm and Fermi wave vector  $k_F$  the spins can be coupled ferromagnetically or antiferromagnetically. By means of flux  $\phi$  one can control the strength of the interaction but does not switch between them. For this reason it is sufficient to discuss three typical situations, for which we are able to get analytic results. These three cases are classified by the value of the RKKY coupling constant: (i) the uncorrelated local-spin case ( $|J_{\text{RKKY}}(\phi)| \ll T$ ), (ii) the ferromagnetic coupling case ( $-J_{\text{RKKY}}(\phi) \gg T$ ), and (iii) the antiferromagnetic coupling ( $J_{\text{RKKY}}(\phi) \gg T$ ). These cases are explained below.

(i) Uncorrelated local-spin limit is realized for high temperature  $|J_{\text{RKKY}}(\phi)| \ll T$  or for the flux  $\phi \approx \pi + 2\pi n$  since then, according to Eq. (5), the RKKY interaction is weak,

$J_{\text{RKKY}}(\phi) \rightarrow 0$ . In this case, the local-spin state is distributed with equal probability among a singlet state and a triplet state  $P_1 \approx P_0 \approx 1/4$  [see Eq. (17)]. The conductance is expressed as

$$\frac{G}{G_K} \approx (\pi\bar{J})^2 \left\{ v^2(1 + \cos\phi \cos^2 k_F l) + 3 \left( 1 + 4\bar{J} \ln \frac{2e^\gamma D}{\pi T} \right) \right\}, \quad (18)$$

where  $G_K = e^2/h$  is the quantum conductance. The first term, which is proportional to  $v^2$  and thus independent of spin-flip processes, is attributed to the phase coherent component of the cotunneling process. It shows the ordinary AB oscillations. The second term in Eq. (18), which is related to spin-flip processes (does not depend on  $\phi$ ), forms the background of AB oscillations. We can see that with decreasing of temperature the Kondo correlations enhance the background: The second term can be interpreted as the parallel conductance through two independent spin- $\frac{1}{2}$  local moments whose conductance is enhanced by Kondo correlations.<sup>28</sup> In the third-order contribution in  $\bar{J}$  in Eq. (18), there is no interference related to the orbital phase  $k_F l$ , which was pointed out by Beal-Monod.<sup>16</sup> We explicitly showed by Eq. (18) that there is also no interference related to the AB phase in the third-order contribution.

(ii) The ferromagnetic coupling,  $-J_{\text{RKKY}}(\phi) \gg T$ : In this case, two local spins form a triplet state  $P_1 \approx 1/3$  and  $P_0 \approx 0$  [see Eq. (17)]. Thus, the conductance is that of  $S=1$  Kondo model plus the potential scattering. For the case of long distance between QD's ( $k_F l \gg 1$ ),

$$\frac{G}{G_K} \approx 2(\pi\bar{J})^2 \left[ 4\bar{J} \cos^2 k_F l \cos^2 \frac{\phi}{2} \ln \frac{2T^*}{\pi T} + \left( 1 + \frac{v^2}{2} + 2\bar{J} \ln \frac{2e^\gamma D}{\pi T} \right) (1 + \cos\phi \cos^2 k_F l) \right]. \quad (19)$$

For the opposite case,  $k_F l \ll 1$ , we obtain the same equation as Eq. (19) with replacing  $T^*$  in the logarithm by  $e^{-\gamma} D$ . The striking feature is that as opposed to the case (i), the Kondo correlations enhance the oscillatory component as it is shown in the second term of Eq. (19). Loosely speaking, two spins are no longer independent phase-breaking scatterers because they “observe” each other and the Kondo correlations enhance the AF coupling of each QD spin to the conducting electrons spins. The first term of Eq. (19) shows the logarithmic divergence, whose cutoff energy is equal to the characteristic temperature of the orbital phase coherence  $T^*$ . This term appears because the spin-1 moment stretches over  $l$ . Using Eq. (19), we can relate the F coupling of spins by RKKY interaction [Fig. 2(a)] with the maximum in the conductance [Fig. 2(c)] around integer values of  $k_F l / \pi$ .

(iii) The antiferromagnetic coupling,  $J_{\text{RKKY}}(\phi) \gg T$ : In this case two local moments form a singlet state  $P_1 \approx 0$  and  $P_0 \approx 1$  [see Eq. (17)]. As the singlet state is decoupled from lead electrons, i.e., electrons flowing through QD's cannot

excite local spins to a triplet state, so only the potential scattering process contributes to the conductance:

$$G/G_K \approx (\pi\bar{J})^2 v^2 (1 + \cos \phi \cos^2 k_F l). \quad (20)$$

Because we consider the Coulomb blockade regime, the cotunneling current is very small. It is the reason why the conductance is suppressed around each half-integer value of  $k_F l / \pi$  [Fig. 2(c)], where the RKKY coupling is antiferromagnetic [Fig. 2(a)]. Here we note that situations (ii) and (iii) are not realized for the flux  $\phi \approx \pi + 2\pi n$  since  $J_{\text{RKKY}}(\phi)$  is small there and the limit (i) is approached. For  $|J_{\text{RKKY}}(0)| > T$  by means of the flux  $\phi$  we can tune between (ii) and (i), or (iii), and (i) but not between (ii) and (iii) situations.

### C. $\phi$ dependence, numerical results

For above three cases, we obtained simple analytic results and clarified that the local-spin state due to RKKY interaction causes the pronounced effect on the conductance. Next, we will analyze the conductance of the system for the full range of the flux  $\phi$  and discuss the additional structures caused by the flux dependent RKKY interaction, which can be an evidence of the RKKY interaction in our system. Figures 3(1-a) and 3(2-a) show the RKKY coupling constant  $J_{\text{RKKY}}(\phi)$  as a function of the flux  $\phi/(2\pi)$ . The former shows plot for F coupling case ( $k_F l / \pi$  is an integer) and the latter shows the plot for AF coupling case ( $k_F l / \pi$  is a half integer). The panels (1-b) and (2-b) are the corresponding plots of the probability for the singlet state for various temperatures, and the panels (1-c) and (2-c) are plots of the conductance. For parameters used in Fig. 3, the Kondo temperature is approximately  $T_K/D \approx 3.7 \times 10^{-6}$ . In the vicinity of zero flux  $\pi = 0$ , electron wave functions constructively interfere and thus the maximum RKKY interaction is induced [panels (1-a) and (2-a)]. For F coupling case, a triplet state is formed, i.e.,  $P_0 \sim 0$ , at low temperature [panel (1-b)] and thus the conductance is enhanced [panel (1-c)] as discussed in case (ii). For AF coupling case at low temperature, a singlet is formed [panel (2-b)] and the conductance is suppressed [panel (2-c)] as it was discussed in case (iii). At half flux, electron wave functions destructively interfere and the RKKY interaction is switched off [panels (1-a) and (2-a)]. Surprisingly at half flux we can observe the maximum in the conductance for both situations F and AF. According to discussion in case (i), this maximum is caused by the term in Eq. (18), which does not depend on the flux and which corresponds to incoherent transport through the two independent spin- $\frac{1}{2}$  local moments related to Kondo correlations. Especially for AF coupling case, it leads to the effective phase shift of AB conductance oscillations by  $\pi$  [panel (2-c)].

In order to compare our results with the limit, where the RKKY interaction is negligible, we show curves of AB oscillations for  $|J_{\text{RKKY}}(\phi)| \ll T$  in panels (3) and (4). As discussed in case (i), the component of the ordinary AB oscillations is very small. The Kondo correlations only enhance the background and they do not promote characteristic structures as the case of the AF or F coupling.

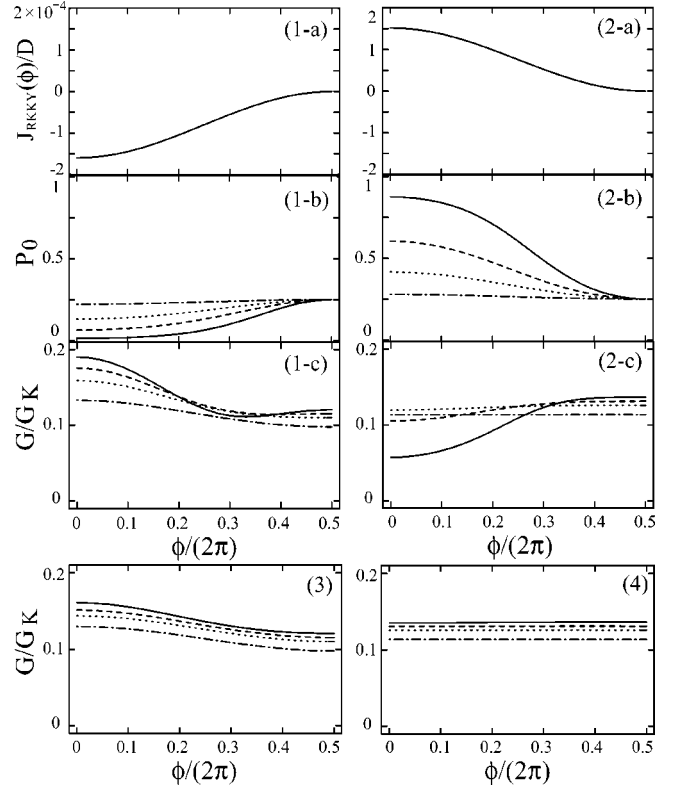


FIG. 3. Flux dependent RKKY coupling constant [(1-a) and (2-a)] probability for singlet state [(1-b) and 2-b)], and conductance [(1-c) and 2-c)], for  $\bar{J}=0.04$ . Panels (1-a), (1-b), and (1-c) correspond to the F coupling case ( $k_F l / (2\pi) = 5$ ) and panels (2-a), (2-b), and (2-c) correspond to the AF coupling case [ $k_F l / (2\pi) = 5.25$ ]. Flux dependent conductance for (3)  $k_F l / (2\pi) = 50$  and (4) 50.25. The solid, dashed, dotted, and dot-dashed lines show the results for  $T/D = 5 \times 10^{-5}$ ,  $10^{-4}$ ,  $2 \times 10^{-4}$ , and  $10^{-3}$ , respectively.

Here we will make a note on the Onsager symmetry. For the two-terminal geometry, it means that the conductance is an even function of the flux. We can see that the RKKY coupling constant  $J_{\text{RKKY}}(\phi)$  is an even function of the flux [Eq. (5)]. This property depends only on the symmetry of the Hamiltonian under the inversion of time and magnetic field<sup>29</sup> and does not depend on the assumption of the mirror symmetry.

## IV. DISCUSSION

### A. Relation to experiments

Here we note some features to distinguish experimentally the RKKY dominant oscillations from the ordinary AB oscillations. The first feature is the characteristic temperature below which the oscillations can be observed: The characteristic temperature of the ordinary AB oscillations  $T^*$  is higher than that of RKKY dominant oscillations  $|J_{\text{RKKY}}(0)|$  by the factor  $\sim \bar{J}^{-2}$ . One can point out that the RKKY dominant oscillations are sensitive to the temperature. The second feature is the temperature dependence of the amplitude of oscillations: Suppose we decrease the temperature from enough

high temperature  $T \gg |J_{\text{RKKY}}(0)|$ , where singlet and triplet probabilities are  $P_1 \approx P_3 \approx 1/4$  and the conductance is expressed by Eq. (18). As temperature is lowered, singlet and triplet probabilities are modified as  $P_0 \approx 1/4[1 - 3J_{\text{RKKY}}(\phi)/(4T)]$  and  $P_1 \approx 1/4[1 + J_{\text{RKKY}}(\phi)/(4T)]$ . Therefore, the correction depending on both the orbital phase and the AB phase,

$$\delta G \approx -(\pi\bar{J})^2 \left\{ 3 \left( 1 + 4\bar{J} \ln \frac{2e^{\gamma}D}{\pi T} \right) (2 + \cos^2 k_{\text{F}}l \cos \phi) + 2v^2(1 + \cos^2 k_{\text{F}}l \cos \phi) \right\} \frac{J_{\text{RKKY}}(\phi)}{4T},$$

emerges. It grows as  $\propto (\ln T)/T$ ; the logarithmic correction is related to the Kondo correlations. We expect that with the help of the Kondo correlations one can distinguish the RKKY dominant AB conductance oscillations from the ordinary AB oscillations.

We also should make a note on our assumptions. In our calculation, we assumed the single-channel leads, however in real experimental situation there could be several channels. As discussed in Ref. 30, for the  $N$ -channel case, the oscillatory component of the conductance decreases approximately as  $1/N$ . From the same discussion it occurs that the coupling constant  $J_{\text{RKKY}}(\phi)$  of RKKY interaction, Eq. (5), will be enhanced approximately by  $N$ .

In Sec. II A, we also assumed the parity symmetry in order to get the simpler expressions. The lack of the symmetry along the vertical axis will reduce the oscillatory component as a function of AB phase in Eq. (5). The symmetry along the horizontal axis is important in order to get compact expressions for the partial self-energy, Eqs. (12)–(14). The deviation from this symmetry will mainly affect the orbital phase, which in turn can modify details of both the RKKY oscillations and the conductance oscillations. However such deviation will not change the general features of the conductance oscillations, i.e., the oscillations dominated by the flux dependent RKKY interaction.

### B. Parameters

Finally we discuss on parameters. For a 2DEG system at an AlAs/GaAs heterostructure, the carrier density of which is typically  $3.8 \times 10^{15} \text{ m}^{-2}$ ,<sup>6</sup> the Fermi energy and the Fermi wave length are  $\varepsilon_{\text{F}} \approx D \approx 14 \text{ meV}$  and  $2\pi/k_{\text{F}} \approx 40 \text{ nm}$ , respectively. The RKKY coupling constant  $J_{\text{RKKY}}(0) \sim \bar{J}^2 D / (k_{\text{F}}l)$  should be larger than the Kondo temperature  $T_{\text{K}} \sim D \exp\{-1/(2\bar{J})\}$ ,  $|J_{\text{RKKY}}(0)| \gg T_{\text{K}}$ , otherwise each spin- $\frac{1}{2}$  local moment forms Kondo singlet and is screened out and thus the RKKY interaction is unimportant. In our calculations, we put  $\bar{J} = 0.04$  which gives the small Kondo temperature,  $T_{\text{K}} \sim 3.7 \times 10^{-6} D \ll |J_{\text{RKKY}}(0)|$ . Because we adopted the perturbation theory, the temperature should be above the Kondo temperature,  $T \gg T_{\text{K}}$ . In order to obtain the large RKKY interaction  $J_{\text{RKKY}}(0) \geq T$  we put the size of the ring as  $k_{\text{F}}l \approx 10\pi$  (about 200 nm).

For a small AB ring, the Zeeman splitting could become important. In order to reduce the Zeeman splitting  $E_{\text{Z}}$  keeping the number of fluxes constant, one could increase the size of the AB ring because  $J_{\text{RKKY}}(0)/E_{\text{Z}} \sim l$ . In such a case, the consideration of the Kondo regime (unitary limit),  $T \lesssim T_{\text{K}}$ , could be necessary because the RKKY interaction was also reduced so the limit  $T_{\text{K}} \geq |J_{\text{RKKY}}(0)|$  was approached. Another way to reduce or to remove the Zeeman splitting is to utilize materials with small Landé  $g$  factor: Such situations are realized in AlGaAs parabolic quantum wells<sup>31,32</sup> or can be achieved by manipulation of the electron wave-function position in 2DEG by means of the gate voltage.<sup>33</sup>

### V. SUMMARY

In conclusion, we have theoretically investigated the RKKY interaction acting between local spins, i.e., two QD's with odd numbers of electrons in CB regime, embedded in the AB ring. We assumed the parity symmetry of the system and such an assumption does not change the result qualitatively. We calculated the RKKY coupling constant and the conductance above the Kondo temperature,  $T > T_{\text{K}}$ , but in the regime where Kondo correlations had already become important. The RKKY coupling constant, the sign of which oscillates as a function of the distance, also depends on the flux and the distance between two QD's. When the RKKY interaction is ferromagnetic, two local spins form a triplet state around zero flux, where the electron wave constructively interferes, and thus the maximum RKKY interaction is induced. As the temperature decreases, the amplitude of AB oscillations is enhanced by Kondo correlations, which is the distinctive difference between the ordinary AB oscillations and those of the ferromagnetically coupled two local spins. The maximum was found at half flux where the RKKY interaction is switched off and the conductance is described by the parallel conductance of two independent spin- $\frac{1}{2}$  local moments whose conductance is enhanced by Kondo correlations. When the RKKY interaction is AF, the phase of AB oscillations is shifted by  $\pi$ . It is because around zero flux, where we obtain the maximum AF interaction, two local spins form a singlet state, which is decoupled from the lead electrons.

*Note added.* After submission of this work, we learned that the RKKY interaction between two QD's was observed experimentally in a different geometry.<sup>34</sup>

### ACKNOWLEDGMENTS

We would like to thank J. Barnaś, V. Dugaev, H. Ebisawa, J. König, S. Maekawa, C. M. Marcus, T. P. Pareek, and G. Schön for valuable discussions and comments. J.M was supported by the DFG under the CFN, ‘‘Spintronics’’ RT Network of the EC Grant No. RTN2-2001-00440, Project No. PBZ/KBN/044/P03/2001, and by the Center of Excellence for Magnetic and Molecular Materials for Future Electronics within the EC Contract No. G5MA-CT-2002-04049. P.B was supported by BMBF (Grant No. 01BM924). H.I was supported by MEXT, Grant-in-Aid for Scientific Research on the Priority Area ‘‘Semiconductor Nanospintronics’’ under

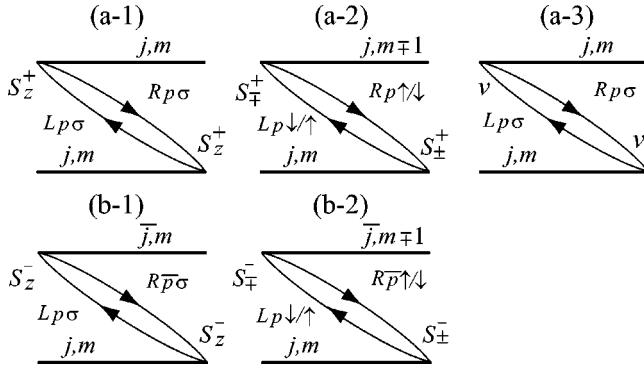


FIG. 4. The diagrams for the second-order partial self-energy representing the transition preserving total-spin quantum number  $j$  [(a-1), (a-2), and (a-3)] and the singlet-triplet transition [(b-1) and (b-2)]. Directed lines represent propagators for lead electrons. Thick solid lines on the Keldysh contour (two horizontal lines) represent propagators for the local spins.

Grant No. 14076204, Grant-in-Aid for Scientific Research (C), Grant No. 14540321, and NAREGI Nanoscience Project.

### APPENDIX: THIRD-ORDER PERTURBATION THEORY

In this appendix, we present detailed calculations of the third-order partial self-energy in terms of  $\bar{J}$  on the basis of the diagrammatic technique in the real-time domain.<sup>25,26</sup> Figure 4 shows the second-order diagrams for the partial self-energy representing the transition preserving the total-spin quantum number  $j$ ,  $\Sigma_{jj}^{LR}$  [(a-1), (a-2), and (a-3)] and the singlet-triplet transition,  $\Sigma_{jj}^{LR}$  ( $j=0,1$ ) [(b-1) and (b-2)]. Green functions of lead electrons are represented by directed solid lines, which are also called “reservoir lines,” and solid lines on the Keldysh contour (two horizontal lines) represent propagators of local spins. Here diagrams (a-1) and (a-3) represent different processes. For the former case, we must count factor  $-1$  for the vertex denoted with  $S_z^+$  when  $\sigma = \downarrow$ . We omitted diagrams which could be obtained by applying the mirror rule.<sup>35</sup>

Following the rules in Ref. 25, the diagram (a-1) plus its mirror diagram can be calculated as

$$\begin{aligned} \Sigma_{jj}^{LR(a-1)} = & \sum_{\substack{p=\pm \\ -j \leq m \leq j}} \frac{i\pi}{8} \int d\varepsilon \gamma_{pL}^+(\varepsilon) \gamma_{pR}^-(\varepsilon) \\ & \times \cos^2 \frac{\phi}{2} \text{Re} \langle j, m | 2(S_z^+)^2 | j, m \rangle. \end{aligned} \quad (\text{A1})$$

The results for the diagrams (a-2) and (a-3), which we term  $\Sigma_{jj}^{LR(a-2)}$  and  $\Sigma_{jj}^{LR(a-3)}$ , can be obtained from Eq. (A1) by changing  $2(S_z^+)^2$  to  $S_\pm^+ S_\mp^+$  and to  $2v^2$ , respectively. In the same way, the diagram (a) plus its mirror diagram is calculated as

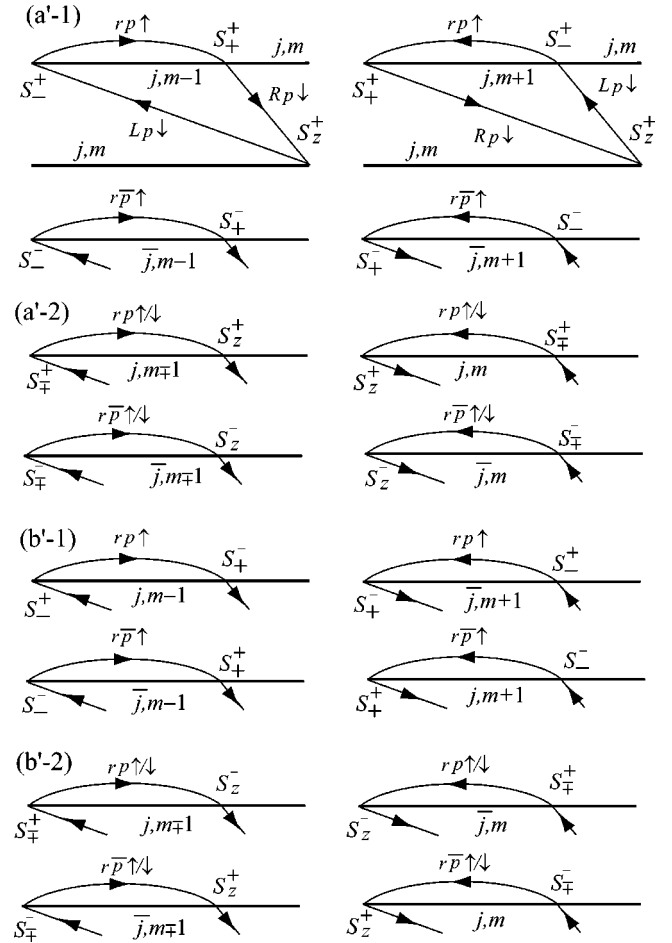


FIG. 5. The third-order diagrams: Each four diagrams of (a'-1), (a'-2), (b'-1), and (b'-2) show corrections for the vertex on the upper branch of the diagram (a-1), (a-2), (b-1), and (b-2) in Fig. 4, respectively.

$$\begin{aligned} \Sigma_{jj}^{LR(b-1)} = & \sum_{\substack{p=\pm \\ -j \leq m \leq j}} \frac{i\pi}{8} \int d\varepsilon \gamma_{pL}^+(\varepsilon) \gamma_{pR}^-(\varepsilon - \Delta_{j\bar{j}}) \\ & \times \cos^2 \frac{\phi}{2} \text{Re} \langle j, m | 2(S_z^-)^2 | j, m \rangle, \end{aligned} \quad (\text{A2})$$

where  $\Delta_{j\bar{j}}$  is the energy difference between the total-spin quantum number  $j$  state and  $\bar{j}$  state. The result for the diagram (b-2), which we denote by  $\Sigma_{jj}^{LR(b-2)}$ , is obtained from Eq. (A2) by replacing  $2(S_z^-)^2$  by  $S_\pm^+ S_\mp^+$ .

The third-order diagrams give the vertex correction to the second-order diagrams. Figures 5(a'-1), 5(a'-2), 5(b'-1), and 5(b'-2) show the correction for the vertex on the upper branch of diagrams (a-1), (a-2), (b-1), and (b-2) in Fig. 4, respectively. Except for the topmost two diagrams, we omitted the lower branch of each diagram, which is exactly the same as for the corresponding diagram in Fig. 4. The left diagrams and the right diagrams show direct tunneling processes and exchange processes, respectively. We did not show the correction for the diagram (a-3) of Fig. 4 because it is proportional to  $\sum_{-j \leq m \leq j} \langle j, m | S_z^+ | j, m \rangle$  and thus vanishes.

For example, the topmost two diagrams in Fig. 5 plus their mirror diagrams are calculated by utilizing the commutation relations, Eq. (10), as

$$\begin{aligned} & \Sigma_{jj}^{LR(a-1)\text{correction}} \\ &= \frac{2i}{4^3} \text{Im} \sum_{rp} \int d\varepsilon_1 d\varepsilon_2 d\varepsilon_3 \frac{\gamma_{Lp}^+(\varepsilon_1) \gamma_{Rp}^-(\varepsilon_3)}{\varepsilon_1 - \varepsilon_3 + i\eta} \cos^2 \frac{\phi}{2} \\ & \quad \times \langle j, m | S_z^+ \left\{ \frac{\gamma_{rp}^-(\varepsilon_2) S_+^+ S_-^+}{\varepsilon_1 - \varepsilon_2 + i\eta} - \frac{\gamma_{rp}^+(\varepsilon_2) S_-^+ S_+^+}{\varepsilon_2 - \varepsilon_3 + i\eta} \right\} | j, m \rangle \\ &= \frac{i\pi}{8} \sum_p \int d\varepsilon \gamma_{Lp}^+(\varepsilon) \gamma_{Rp}^-(\varepsilon) \cos^2 \frac{\phi}{2} \\ & \quad \times \text{Re} \left\{ \frac{\sigma_{1p}(\varepsilon)}{4} \langle j, m | 2(S_z^+)^2 | j, m \rangle \right\}, \end{aligned} \quad (\text{A3})$$

where  $\sigma_{1p}$  is defined in Eq. (15). Here we counted the minus sign for a loop with three vertices in the anticlockwise direction and we dropped terms except for the renormalization of the transmission probability. We checked that terms which we dropped are canceled out by the diagrams other than those depicted in Fig. 5, i.e., diagrams in which the position of a lower vertex is in between upper two vertices. Further we neglected the integral  $\text{Re} \int d\varepsilon' \gamma_p(\varepsilon') / (\varepsilon + i\eta - \varepsilon')$  which is at most  $\sim \mathcal{J}\varepsilon/D$  for  $k_{Fl} \ll 1$  or  $\sim \mathcal{J}\{|\varepsilon|/D + 1/(k_{Fl})\}$  for  $k_{Fl} \gg 1$ . By adding Eqs. (A1) and (A3), we obtain Eq. (A1) with replacing  $2(S_z^+)^2$  by  $2[1 + \sigma_{1p}(\varepsilon)/4](S_z^+)^2$ .

Other two diagrams in panel (a'-1) of Fig. 5 can be calculated in the same way. In Fig. 5 we omitted diagrams obtained by reversing direction and indices for spin and lead of reservoir lines. By calculation of all such diagrams and adding them to Eq. (A1), we obtain Eq. (A1) with replacing  $2(S_z^+)^2$  by  $2z'_{jj}(S_z^+)^2$ , where the renormalization factor is given by

$$z'_{jj} = 1 + \frac{1}{2} \left\{ \sigma_{1p}(\varepsilon) + \frac{\sigma_{1p}(\varepsilon - \Delta_{\bar{j}j}) + \sigma_{1p}(\varepsilon - \Delta_{j\bar{j}})}{2} \right\}. \quad (\text{A4})$$

In Fig. 5 we did not show the lower vertex corrections, which are given in the same way as the upper vertex corrections. By counting lower vertex corrections,  $z'_{jj}$  is modified as

$$z_{jj} = 1 + \sigma_{1p}(\varepsilon) + \frac{\sigma_{1p}(\varepsilon - \Delta_{\bar{j}j}) + \sigma_{1p}(\varepsilon - \Delta_{j\bar{j}})}{2}. \quad (\text{A5})$$

Finally, the third-order contributions change  $\Sigma_{jj}^{LR(a-1)}$  to  $\Sigma_{jj}^{LR(a-1)(2)}$ , where the latter is obtained from the former by replacing  $2(S_z^+)^2$  with  $2z_{jj}(S_z^+)^2$ . For the diagrams other than those of panel (a'-1) of Fig. 5, we can repeat the same discussions as above. The result for diagrams (a-2) and (a'-2) of Figs. 4 and 5, respectively, and their derivative diagrams, which we term  $\Sigma_{jj}^{LR(b-2)(2)}$ , is obtained from Eq. (A1) by replacing  $2(S_z^+)^2$  with  $z_{jj} S_+^+ S_-^+$ .

By calculating diagrams (b'-1) of Fig. 5 and their derivative diagrams, and adding them to the diagram (b-1) of Fig. 4, we obtain  $\Sigma_{jj}^{LR(b-1)(2)}$ , which is the same expression as Eq. (A2) with replacing  $2(S_z^-)^2$  by  $2z_{j\bar{j}}(S_z^-)^2$ . Here

$$z_{j\bar{j}} = 1 + \sigma_{1p}(\varepsilon) + \sigma_{1\bar{p}}(\varepsilon - \Delta_{\bar{j}j}). \quad (\text{A6})$$

The result for the diagrams (b-2) and (b'-2) of Figs. 4 and 5, respectively, and their derivative diagrams, which we term  $\Sigma_{j\bar{j}}^{LR(b-2)(2)}$  is obtained from Eq. (A2) by replacing  $2(S_z^-)^2$  with  $z_{j\bar{j}} S_+^+ S_-^+$ . Finally, by summarizing  $\Sigma_{jj}^{LR(a-1)(2)}$ ,  $\Sigma_{jj}^{LR(a-2)(2)}$ , and  $\Sigma_{jj}^{LR(a-3)}$ , we obtain the first term of Eq. (12) for  $j=1$  and the first term of Eq. (13) for  $j=0$ . By adding  $\Sigma_{j\bar{j}}^{LR(b-1)(2)}$  to  $\Sigma_{j\bar{j}}^{LR(b-2)(2)}$ , we obtain the first term of Eq. (14).

For now, we have explained only the diagrams related to the time-reversal symmetric term, corresponding to the first and second lines in Eq. (11). Diagrams related to the time-reversal symmetry breaking term, the third line in Eq. (11), are obtained from Figs. 4 and 5 by changing the parity indices of the right reservoir lines. For example, the corresponding diagram of (a-1) of Fig. 4 is calculated as

$$\begin{aligned} \Sigma_{jj}^{LR(\widetilde{a-1})} &= \sum_{\substack{p=\pm \\ m=\pm 1,0}} \frac{i\pi}{8} \int d\varepsilon \gamma_{pL}^+(\varepsilon) \gamma_{\bar{p}R}^-(\varepsilon) \sin^2 \frac{\phi}{2} \\ & \quad \times \text{Re} \langle j, m | 2(S_z^+)^2 | j, m \rangle. \end{aligned} \quad (\text{A7})$$

For vertex corrections, the change in the parity indices of the right reservoir lines corresponds to the operation of the replacement of  $\sigma_{1p}$  by  $\sigma_{0p}$ . Thus the second terms of Eqs. (12)–(14) can be obtained from first terms by replacing  $\sigma_{1p}$ ,  $\cos^2(\phi/2)$ , and  $\gamma_{p(\bar{p})R}^-$  with  $\sigma_{0p}$ ,  $\sin^2(\phi/2)$ , and  $\gamma_{p(p)R}^-$ , respectively.

<sup>1</sup>C. Kittel, *Solid State Physics* (Academic Press, New York, 1968), Vol. 22, pp. 1–26.

<sup>2</sup>*Spin Dependent Transport in Magnetic Nanostructures*, edited by S. Maekawa and T. Shinjo, *Advances in Condensed Matter Science* Vol. 3 (Taylor & Francis, London, 2002).

<sup>3</sup>P. Bruno, *Phys. Rev. B* **52**, 411 (1995).

<sup>4</sup>A.W. Holleitner, C.R. Decker, H. Qin, K. Eberl, and R.H. Blick, *Phys. Rev. Lett.* **87**, 256802 (2001).

<sup>5</sup>A. Yacoby, M. Heiblum, D. Mahalu, and H. Shtrikman, *Phys. Rev. Lett.* **74**, 4047 (1995).

<sup>6</sup>K. Kobayashi, H. Aikawa, S. Katsumoto, and Y. Iye, *Phys. Rev. Lett.* **88**, 256806 (2002).

<sup>7</sup>D. Loss and E.V. Sukhorukov, *Phys. Rev. Lett.* **84**, 1035 (2000).

<sup>8</sup>A. Georges and Y. Meir, *Phys. Rev. Lett.* **82**, 3508 (1999).

<sup>9</sup>J. König and Y. Gefen, *Phys. Rev. Lett.* **86**, 3855 (2001).

<sup>10</sup>J. König and Y. Gefen, *Phys. Rev. B* **65**, 045316 (2002).

<sup>11</sup>C. Bruder, R. Fazio, and H. Schoeller, *Phys. Rev. Lett.* **76**, 114 (1996).

<sup>12</sup>Y. Gefen, Y. Imry, and M.Y. Azbel, *Phys. Rev. Lett.* **52**, 129 (1984).

- <sup>13</sup>As addressed in detail recently (Ref. 21), even for the case of noninteracting QD's, the relation between two approaches is not obvious.
- <sup>14</sup>C. Jayaprakash, H.R. Krishna-murthy, and J.W. Wilkins, Phys. Rev. Lett. **47**, 737 (1981).
- <sup>15</sup>G. Hackenbroich and H.A. Weidenmüller, Phys. Rev. Lett. **76**, 110 (1996).
- <sup>16</sup>M.T. Beal-Monod, Phys. Rev. **178**, 874 (1969).
- <sup>17</sup>B.A. Jones and C.M. Varma, Phys. Rev. Lett. **58**, 843 (1987).
- <sup>18</sup>B.A. Jones, C.M. Varma, and J.W. Wilkins, Phys. Rev. Lett. **61**, 125 (1988).
- <sup>19</sup>B.A. Jones, B.G. Kotliar, and A.J. Millis, Phys. Rev. B **39**, 3415 (1989).
- <sup>20</sup>N.F. Schwabe, R.J. Elliott, and N.S. Wingreen, Phys. Rev. B **54**, 12 953 (1996).
- <sup>21</sup>B. Kubala and J. König, Phys. Rev. B **67**, 205303 (2003).
- <sup>22</sup>Y. Yafet, Phys. Rev. B **36**, 3948 (1987).
- <sup>23</sup>A.C. Hewson, *The Kondo Problem to Heavy Fermions* (Cambridge University Press, Cambridge, UK, 1993).
- <sup>24</sup>K. Matho and M.T. Beal-Monod, Phys. Rev. B **5**, 1899 (1972).
- <sup>25</sup>H. Schoeller and G. Schön, Phys. Rev. B **50**, 18 436 (1994).
- <sup>26</sup>J. König, J. Schmid, H. Schoeller, and G. Schön, Phys. Rev. B **54**, 16 820 (1996).
- <sup>27</sup>H. Akera, Phys. Rev. B **47**, 6835 (1993).
- <sup>28</sup>Equation (18) recovers a previous result for single impurity (Ref. 36). Namely, Eq. (18) with dropping the factor  $\ln(2e^{\gamma}/\pi)$  and also the flux and length dependent terms is twice as large as Eq. (27) in Ref. 36, which corresponds to the transport through two independent impurities. In our notations  $\bar{J}$  and  $D$  correspond to  $\nu \mathcal{J}_{rr'}^{(0)}(r, r'=L,R)$  and  $D_0$  in Ref. 36, respectively.
- <sup>29</sup>R. Kubo, M. Toda, and N. Hashitsume, *Statistical Physics II*, Springer Series in Solid-State Sciences Vol. 31 (Springer-Verlag, Berlin, 1985).
- <sup>30</sup>M. Büttiker, Y. Imry, R. Landauer, and S. Pinhas, Phys. Rev. B **31**, 6207 (1985).
- <sup>31</sup>G. Salis, Y. Kato, K. Ensslin, D.C. Driscoll, A.C. Gossard, and D.D. Awschalom, Nature (London) **414**, 619 (2001).
- <sup>32</sup>G. Lindemann, T. Ihn, T. Heinzel, K. Ensslin, K. Maranowski, and A.C. Gossard, Photonics Spectra **13**, 638 (2002).
- <sup>33</sup>H.W. Jiang and E. Yablonovitch, Phys. Rev. B **64**, 041307 (2001).
- <sup>34</sup>C.M. Marcus *et al.* (private communication).
- <sup>35</sup>J. König, *Quantum Fluctuations in the Single-Electron Transistor* (Shaker, Aachen, 1999).
- <sup>36</sup>A. Kaminski, Yu.V. Nazarov, and L.I. Glazman, Phys. Rev. B **62**, 8154 (2000).